Fullerene, Carbon Nanotubes and Graphene: A comprehen-sive review

Sunila Bakhsh

Dept of Physics, Balochistan University of Information Technology Engineering and Management Sciences Quetta, Pakistan, sunila.bakhsh@buitms.edu.pk

Recommended Citation

Fullerene, Carbon Nanotubes and Graphene: A comprehen-sive review

Abstract

The aim of this review is to provide an update on the present status of carbon allotropes, namely fullerenes, carbon nanotubes, and graphene, with a focus on various structures that result from changes in carbon bonding. This review will also help us understand the main features, processes and advancement in the study of fullerene, CNTs and graphene. The extraordinary mobility that is extremely sensitive to field effect makes graphene an appealing substitute to CNTs in FET-based applications. For this, graphene can also be used to produce sensitive sensors and as coating material.

Keywords

Creative Commons License

REVIEW ARTICLE

Fullerene, Carbon Nanotubes and Graphene: A Comprehensive Review

Sunila Bakhsh

Dept of Physics, Balochistan University of Information Technology Engineering and Management Sciences Quetta, Pakistan

Abstract

The aim of this review is to provide an update on the present status of carbon allotropes, namely fullerenes, carbon nanotubes, and graphene, with a focus on various structures that result from changes in carbon bonding. These nano-carbons can be categorized as sp^2 or sp^3-carbon nanomaterials for bond variations. Fullerene and carbon nanotubes (CNTs) have been studied extensively due to their excellent electrical properties for electrical conductors and semiconductors. In addition, graphene has proven to be stable in all normal conditions and is unaffected by mobilities under standard conditions. This review will also help us understand the main features, processes and advancement in studying fullerene, CNTs and graphene. The extraordinary mobility that is extremely sensitive to field effect makes graphene an appealing substitute to CNTs in FET-based applications. Graphene can also be used to produce sensitive sensors and as a coating material.

Keywords: Carbon nanotubes, Fullerene, Graphene, Single-wall nanotube (SWNT), Multiwall nanotube (MWNT), Nano composites

1. Introduction

The study of pure carbon has gained attention from chemists for being the foundation of life and one of the most abundant elements. The carbon molecules or clusters exhibit distinct characteristics depending on the various forms. The chemical structure and energetics of an element depend on the behaviour of such chemical bonds, which can vary over distances greater than just a few angstroms [1]. To enhance the interaction between neighbouring electrons in the valence shells of atoms and to sustain the stability of the resulting chemical bond, atoms tend to align themselves close to one another. This example is imitated by space-filling models, which see the coinciding electronic shells of atoms nearby in a given sample of an element [2].

Linus Pauling became the first man to give the polyhedral and tubular forms of asbestos minerals [3,4]. These included kaolinite, renowned for its ability to form polyhedral structures that are the boron carbon-hydrogen compounds [5], which were later studied by William Lipscomb [6]. Carbon has an atomic number of 6, with $1s^2$, $2s^2$ and $2p^2$ electronic configuration [7]. In the case of graphite, the bonds are formed between one carbon atom and its three neighbouring atoms from $2s$, $2p_x$ and $2p_y$ shells. The atomic structure of carbon in graphite exhibits anisotropy and demonstrates partially metallic properties in the semi-metallic behaviour. Additionally, it has been observed that graphite has low electrical conductivity. This review discusses the various allotropic forms of carbon (Fig. 1), including fullerene, graphene, and carbon nanotubes (CNTs), their properties and applications. Graphene has a unique structure consisting of a single planar sheet of fused carbon atoms [8−10]. This structure is still somewhat enigmatic and has led to the development of new theoretical predictions for single-walled carbon nanotubes (SWNTs) [11−13].

Currently, these predictions are getting support through new experiments [14,15]. Following the way of rolling the sheets, the SWNT can either be metallic or semiconducting. The latter can have either a small or moderate gap, depending on their
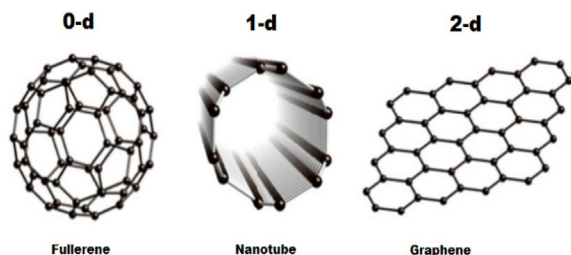
Fig. 1. Allotropes of Carbon [17].

configured modifications due to curvature properties depending on their curvature properties resulting from their specific configuration. However, this theoretical understanding breaks down when inherent defects are present in the graphene sheet [16]. These defects significantly alter the electronic structure and other chemical and optical properties of graphene. Understanding SEM images of sp^2-bonded carbon is under an unsettled discussion over how defects display themselves [18].

Another concern here is the chemical reactivity of carbon nanostructures and how this property relates to their other properties. At the nanoscale, electronic structure calculations are essential in the knowledge of the various materials [19], and undeniably the mishmash of theory and simulations has guided the science of carbon nanotubes (CNTs).

C_{60}, among other carbon molecules, has continuously drawn the attention of chemists. The fullerene structure, which resembles a football shape and owns an icosahedral symmetry, is particularly intriguing [20]. New compounds are being developed from the large family of fullerene. The discovery of carbon fullerenes by Kroto, Smalley, and Curl in 1985 [21], subsequently the discovery of carbon nanotubes by Iijima, marked a significant milestone in understanding this realm [22]. The discovery of inorganic nanotubes and fullerene-like structures in 1992 by Adams [19] marked an important milestone in the field of nanoscience and ushered in a new era in the history of inorganic chemistry. It is widely acknowledged that the benefits of fullerenes and CNTs are not limited to carbon alone but can also extend to other two-dimensional layered composites.

2. Fullerene

The proposed structures of fullerene are similar to football. Among them, more than 50% are identical to dome structures with exceptional stability. Fullerene got its name in honour of an American architect as the structure resembled his geodesic domes. C_{60} is the most plentiful archetypal of the

fullerene members. C_{60} was initially produced in 1985 by Kroto and Smalley group at Rice University, leading them to get the Nobel Prize [23]. In their work, they used a graphite resistive heating method to produce C_{60}.

The synthesis of C_{60} at a scale of one-thousandth of a gram led to new avenues of research. However, the investigation of the properties and reactivity of these materials proved to be the most intriguing aspect.

The superconducting behaviour of C_{60} showed that it has vast potential in numerous fields of materials and electronics. The electrochemical performance created hopes for future devices; however, processing the C_{60} molecule was a greater challenge. The difficulty lies in the non-solubility of C_{60} and the coagulation in the solvents. However, it is possible to overcome this problem through a method known as material functionalization [24]. The change in the C_{60} structure, while retaining its distinct characteristics, has facilitated its utilization in numerous applications [25].

2.1. Structure and chemistry of fullerenes

Various structures of fullerene are possible, such as C_{20}, C_{60} and C_{70} [26], the smallest of which is called Buckminsterfullerene or C_{20}. The bonding in all the loops of C_{60} is fused, as shown in Fig. 2, where all the double bonds are conjugated.

Earlier, it was considered to have a polyenic assembly, having double bonds with six atoms in a loop [27]. Various spectroscopy techniques have shown the presence of two dissimilar types of bonds [28]: short (1.39 °A) and long (1.43 °A). Short ones are between two hexagonal loops, while the length between the pentagonal and hexagonal loops combines them into a football shape. The double bonding provides sufficient strain to form a caged structure for C_{60}.
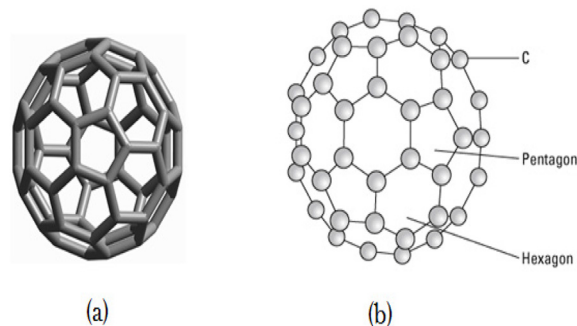

Fig. 2. (a) Fullerene structure similar to a football-like shape (b) C_{60}, the Hexa and Penta surfaces [31].

The change in the angle of sp^2 hybridization (pyramid formation), carbon atoms, puts an extra strain on C_{60}, which causes it to be more reactive [29,30]. In the context of C_{60} and other fullerenes, the hybridization of carbon atoms can be modified to reduce the strain caused by their unique structures. This modification, however, typically requires specific chemical reactions that can alter the bonding arrangements and geometries of the carbon atoms.

For example, geometric shapes comprising 6 and 6 loops can generate many possible assemblies (Fig. 3). Sometimes we use the terminology dihydro fullerenes (DHF), which is specified for the Mono-functionalized fullerenes (MFF) or, sometimes else, organo-fullerene for the addition of organic compounds. Similarly, the open structures of the three-membered structures have an interesting category of functionalized fullerenes.

Wudl and his colleagues [33] were able to produce fulleroid and methane-fullerene structures with a variety of applications, such as photo-conductive material coatings, by adding CH_2N_2 byproducts to C_{60} that helped to produce structures like fulleroids and methane-fullerene, which has a variety of applications like photo conducting material coatings [34].

While a comprehensive mechanism for adding an element to this class has yet to be reached, the promising results ensure the future of fullerenes. And in specific, C_{60} possibly will be utilized as the fundamental block for building complex systems and creating complex molecular structures.

2.2. C_{60} production

The C_{60} is produced by abbreviating carbon vapours, providing a high temperature and keeping the process as slow as possible (Fig. 4).

Highly pure graphite is used as a rod to produce an arc in its synthesis. The assembly is held in the
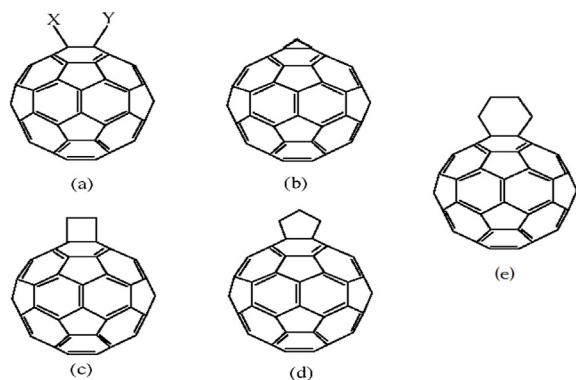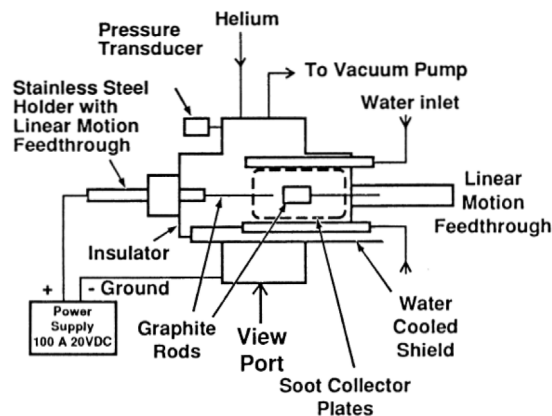

Fig. 4. Apparatus for the fullerenes extraction [35].

helium to decelerate the carbon chains from the graphite rods. This, in turn, gives enough time to generate the preliminary cluster in pentagon assemblies. Keeping the distance of the electrodes constant, the C_{60} is collected from the slurry by dissolving in N-methyl l-2-pyrrolidinone. Approximately more than 90% of dissolvable fullerene can be obtained from such a method.

The limitation of this process is the formation of dangling bonds, which chiefly arise from the extrinsic contamination of elements (e.g. H, H_2O).

2.3. Application of fullerene

Numerous applications of C_{60} are currently under experimentation. Some potential applications use K or Rb impurity-based superconductors in polymers, thin film optics and direct band-gap semi-conductors. The fusion of this material with polymers can provide the polymer that contains the unique structural property and stability of this molecule [36,37]. We can also obtain an electroactive polymer with high optical qualities [27]. It can also provide a suitable coating material for photo-conducting applications like solar collectors and for creating new molecular networks. Thin films comprising this material have gained much attention, ensuring that any material has the characteristics of fullerene by just coating a thin layer on the surface. Currently, SAM and Langmuir's thin layers are widely used as electroactive materials that can exhibit a response to an applied electrical field or current, such as changes in shape, volume, or colour.

3. Carbon nanotubes

The CNTs comprise coaxial manifold layers of walls in a honeycomb lattice. They can be single-

Fig. 3. C_{60} 6,6 junction geometry (a) open structure (b) 3-membered loop (c) 4-membered loop (d) 5-membered loop (e) a 6-membered loop [32].

walled (SWNTs), consisting of a single layer of carbon atoms, or multi-walled (MWNTs), consisting of several concentric layers of carbon atoms. SWNT was manufactured in 1993 from the arc discharge (Fig. 5) on transition metal doped graphite probes [38].

The edges of carbon nanotubes (CNTs) consist of a layer of carbon atoms arranged in a honeycomb lattice, which is similar to graphite but twisted into a cylindrical tube [39,40].

There are three categories of CNTs, depending on the alignment of the six adherent loops in the honeycomb matrix relative to the tube axis: armchair, zigzag, and chiral [41]. Armchair CNTs have unique electronic and mechanical properties suitable for applications such as nanoelectronics and high-strength materials, while zigzag CNTs exhibit magnetic properties and have potential applications in spintronics and nanomagnetic devices. Chiral CNTs have a helical structure and a wide range of electronic and mechanical properties depending on their chirality, making them useful in various applications.

The final category of CNTs exhibits non-symmorphic characteristics, resulting in an asymmetric mirror image. Both empirical and theoretical research has demonstrated that CNTs possess exceptional electrical properties, with their conductivity and semiconducting characteristics being highly dependent on their size and level of symmetry. Moreover, over two-thirds of nanostructures belonging to the zigzag and chiral types exhibit properties similar to that of a semiconductor [42]. Approximately one-third of CNTs, with changes in diameters, and the entirety of armchair nano-assemblies, regardless of their diameter, can conduct electricity similar to that of all metals. This

remarkable characteristic has been instrumental in the development of nanoscale devices.

Collins and Zettl [43] have successfully confirmed the existence of Schottky barriers along carbon nanotubes. The first CNT transistor was introduced in the late 1990s, establishing CNTs as an innovative material that has the potential to drive the development of nano-devices. CNT-based computers also have the capability to transform industries. The upcoming carbon-based computer, expected to emerge in the coming decades, will be significantly small, enhanced processing speed, and exhibit enhanced power.

Well-aligned CNT assemblies can be produced through chemical vapour deposition (CVD) or hydrocarbon pyrolysis fabrication methods. By selecting the proper characteristic ratio and reducing the tip radius of curvature as much as possible, these nanotubes can generate electron beams with exceptional intensity and shallow energy range at low voltages. As a result, CNTs can serve as an economical and straightforward field-emission electron gun in electron microscopy and certain display-based devices.

3.1. Growth of CNTs

Nanotubes were discovered by Sumio Iijima from NEC Company. Iijima models were produced by DC-arc discharge between carbon probes dipped in a noble gas [42]. Wolfgang used a similar device from Max Planck and Don Huffman from the University of Arizona, where the fullerenes were made [44]. Roger Bacon used an electric arc in the 1960s to generate carbon fibres of a suitable thickness [45]. A proposition made by Iijima suggests that carbon nanotubes may have already been formed in earlier experiments but remained undetected due to the lack of high-resolution microscopes at that time [46].

Although various fullerenes can be produced by vaporizing carbon atoms and condensing them into small clusters through different methods, the growth of long tubes can be stimulated by the field created by charges in arc-discharge pulses.

CNTs can be produced by applying a current to the negative electrode, with a deposition rate of approximately 1 mm/min at a high temperature of about $(2-3) \times 10^3$ °C, using I and V within the range of 100A and 20V, respectively. Ajayan and Ebbesen [47] later discovered a more effective method for producing CNTs, involving the addition of transition metals to act as a catalyst and prevent tube-like assemblies from wrapping around and forming smaller fullerene cages. These transition metals also help to reduce the temperature required for CNT
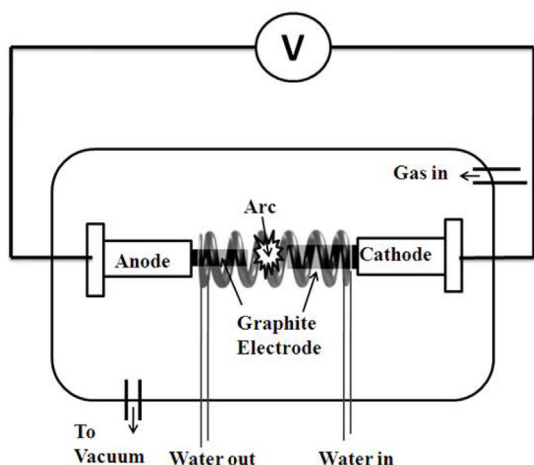
Fig. 5. Synthesis of SWNT from arc discharge method [39].

growth. Without cooling, CNTs can blend and fuse like soap foam.

At Rice University, a significant breakthrough was achieved by condensing a mixture of laser-vaporized carbon (metal-catalyzed arc-discharge method) with transition metals at a temperature range of 1200 °C, resulting in the formation of SWNTs in proportions exceeding 70% [48]. Moreover, these CNTs produced in the condensing vapour are assembled into bundles resembling ropes that are longer than one millimetre, making them highly suitable for engineering applications.

3.2. Structure of CNTs

CNTs, or carbon nanotubes, are large linear molecules composed of curved, convex surfaces exclusively of hexagons and pentagons [49]. The topology of CNTs follows specific rules and results in remarkable properties that differ from their precursor, graphite, which has a hexagonal surface configuration [50]. The process can be initiated by splitting C_{60} and adding ten carbon atoms to create C_{70}, followed by adding another segment to form C_{80}. This process can be repeated to create a bucky tube with infinite length.

Another method involves an expert taking a large piece of 1-atom thick graphite film, removing a layer, and seamlessly stitching it into a cylinder. The expert determines the type of assembly to be used, whether it is a strip-thickness parallel assembly, perpendicular assembly, or an assembly at a specific angle θ based on the desired outcome. The three resulting assembly configurations are zigzag, armchair, and chiral. These configurations are achieved by rotating the entire graphene sheet at an angle between 0 and 30° for the zigzag and chiral configurations. The roll-up vector, expressed as (n, m), determines the alignment direction and specifies the number of steps along the a and b axes. Its integer components solely determine the tube diameter, helicity, and chirality [51]. As we know, the C−C assembly has a length of 0.14 nm; let us proceed with some values like 9 and 0 or 5 and 5 parallel to $\theta = 0$ and $\theta = 30°$) so that bucky tubes ~0.7 nm thick, including the disassociating caps, finish this task. This type of assembly exhibits a specific helicity, which has been demonstrated to be more significant than just the thin cylinder structure of CNTs through diffraction experiments.

The ability of carbon to use its four outermost electrons allows for the occurrence of such assemblies in both the fullerene and graphite families. Three of these electrons bond with a partner, while the fourth is shared among all, known as π. These π bonds give rise to the unique electrical conductivity of certain CNTs. Although the ideal sp^2 arrangement occurs in a flat hexagonal lattice, rolling up the sheet incurs relatively less strain energy, which is later released by saturating the dangling bonds at the periphery of the cylinder [52].

Additionally, such carbon can have more faces in structures (Penta or Hepta). These faces contribute to a natural Gaussian curvature from a geometrical perspective. Penta-assembly results in a structure resembling a cap and is denoted by a plus sign (+), while Hepta-assembly results in a structure resembling a saddle and is denoted by a minus sign (−). The analysis of CNTs and their helical assembly is fundamentally linked to the mechanisms by which they are constructed.

The growth of nested MWNT assemblies can be facilitated by the strained connection between the coaxial peripheries, which are highly flexible and, therefore, available for adding new atoms [53−55]. A high electric field is applied to maintain the open end. The final step involves using nickel-cobalt small clusters at the edges, which appear to be responsible for the large-scale growth of 10 10 tubes [56]. The cluster mixture transforms all unfavourable structures into hexagons and facilitates the continuous growth of a straight cylindrical structure.

3.3. Electrical properties CNTs

The electrical properties of carbon nanotubes (CNTs) are determined by the distribution of electrons within their shells and energy bands. Certain energy levels exhibit symmetrical patterns that are not allowed, resulting in gaps between energy levels that can be accessed by negatively charged particles. The lower energy bands are typically full and stable, while the upper bands are partially filled with negatively charged ions that are able to gain kinetic energy and move in response to an applied electric field. This region of partially filled energy levels is known as the conduction band [42]. The size of the band gap is a critical factor for electronic applications. A wider band gap results in the creation of semiconductors, which are used to produce durable and reliable electronic components. In contrast, a narrow band gap has numerous applications in infrared technology. Graphite sheets, however, do not have a band gap between the occupied and unoccupied states. Instead, a minority of ions are able to move along these sheets.

The wave vector k in carbon nanotubes (CNTs) can only be oriented in one direction, along the lateral axis of the tube, unlike graphene, where it can be oriented in two directions [57]. The

movement of negatively charged ions in carbon nanotubes (CNTs) is restricted to the vertical direction around the tube due to the periodicity of the lattice, limiting their azimuthal freedom to discrete values. These ions remain in a state just below the occupied energy levels, i.e. the Fermi level, which is located at the intersection of the valence and conduction bands. This allows the negatively charged ions to move freely and conduct electricity in the CNT. In contrast, the low density of such carriers in graphite results in poor conductivity. However, the carrier concentration in armchair CNTs is thousands of times greater than that in high-conducting metals. The Peierls effect can cause unexpected fluctuations in conductivity, but in CNTs, a small thermal motion is enough to restore regularity and conductivity.

Dekker was the first to report achievement for such [59]; later attempts were made by Harvard [60]. Using a two-probe arrangement to measure the resistance of carbon nanotubes (CNTs) presents challenges in separating the resistance of the end connections from that of the CNT itself and the Schottky barrier. CNTs are often placed on a substrate with gold pads and connected using either the tip of a microscope probe [58] or lithographically positioned metal leads, as shown in Fig. 6 [61,62]. By allowing current to flow through the carbon nanotube (CNT) and measuring the resulting voltage, the conductivity of the CNT can be quantified and recorded. Changes in resistance due to temperature and magnetic fields can be used to investigate the type of conductance.

Experiments have been conducted to create both metallic and non-metallic CNTs. However, in none of the described assemblies was an increase in
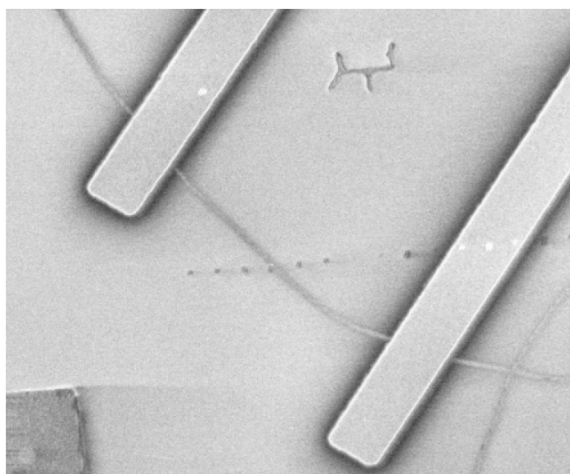

Fig. 6. Metal electrodes covering the CNT are defined in the lithography step [58].

resistivity due to temperature observed, likely due to MWNTs and defects. For armchair CNTs, resistivity increases with temperature, similar to metals. Despite their small size, the perfect arrangement of CNTs provides them with unique properties, including fewer scattering modes for negatively charged ions that are useful in optical communication. In CNTs, the current value (I) surges and drops discretely rather than changing evenly with voltage (V), revealing the grainy behaviour of these quantum wires. This phenomenon was initially caused by the emergence of current from a single CNT, but later experiments showed that it occurs in many CNTs, including those in a 1.4 nm armchair assembly. Apart from their small size, these CNTs appear similar to a field-effect transistor (FET) [63]. The proper arrangement of carbon nanotubes and their complex structural assembly discourages defects and prevents elastic vibrations, allowing for easy movement of electrons between the ends [64]. This behaviour is similar to that of a particle in a box, where the dimensions of the box are small enough to create discrete energy levels for the electrons. Additionally, the charge storage of the box is relatively low, making it difficult to remove an electron.

These factors lead to the significant spacing between the energy levels responsible for conductance. The electrons behave like a boat propelled smoothly from the source to the drain if a slight inclination is provided. This phenomenon occurs only at specific gate voltages that regulate the hierarchy of energy levels, resulting in an array of crests in the current. Even a slight variation in the bias can cause a discrete increase in current, signifying the quantum effect. However, the conduction behaviour of carbon nanotubes is challenging to handle and requires low temperatures (~10K to mK) to mitigate the problem of thermal noise [66,67]. Structural deformation or bending of CNTs (as shown in Fig. 7) can alter the energy levels responsible for conductance, leading to a sharp increase in the electrical signal even in a small circuit.

The conductivity observed in these molecular wires results from carbon achieving the essential characteristics required for metallic behaviour in a crystal lattice [57]. This characteristic is similar to the features that make C_6H_6 aromatic. The π electrons move around the carbon ring without reacting with it, which is unusual for metals. Unlike typical metals, the CNT molecule is an excellent conductor [68]. When impurities are added, the metal molecules become good conductors but can be easily contaminated by contact with air or water.
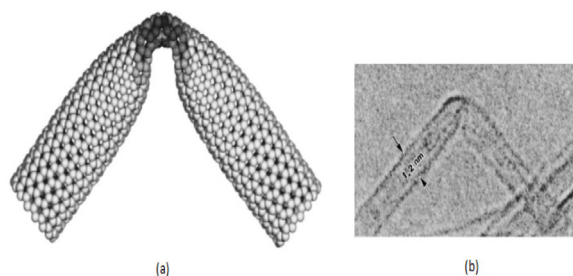
Fig. 7. (a) Computer simulation of bend in the CNT assembly; darker area shows more strained atoms. (b) Bend formed in SWNT of about 1.2 nm diameter [65].

Fig. 8. Single-walled [75] and Multi-walled [76] CNT Structures.

3.4. SWNT assemblies

SWNTs, or single-walled carbon nanotubes, have internal diameters that measure approximately 4 nm. In the early 1990s, a significant development in the field of nanotechnology was made by Iijima and Toshinari Ichihashi when they described the production of SWNTs in their research [69].

This development was groundbreaking because SWNTs exhibited structures that were almost identical to those of perfect nanotubes [70]. Moreover, the discovery of SWNTs was an innovation in the field of nanotechnology. Prior to this, researchers were already aware of catalytically produced multi-walled graphitic tubules and fullerene-based nano-tubes, but the discovery of fullerene-associated nanotubes was made several years later. It is important to note that the appearance of fullerene-associated nanotubes differs significantly from that of MWNT assemblies.

The SWNTs typically have smaller diameters of around 1 nm and can be bowed and looped instead of straight. Contamination with amorphous carbon and catalytic atoms is a common occurrence in the production of SWNTs, but these impurities can also be useful in aiding the production of purer samples [71]. Smalley described an alternative method for preparing SWNTs that was similar to the traditional method for producing carbon [72]. This involved laser-based vaporization of graphite and could produce high yields of SWNTs with consistent diameters. The highly uniform diameters enabled the generation of more aligned assemblies (as shown in Fig. 8) than those made using the arc method. As a result of their research, the Smalley group referred to the aligned assemblies of SWNTs produced using their method as nanotube ropes [56]. Early experiments demonstrated that nanotube rope samples contained a significant proportion of nanotubes with a definite arm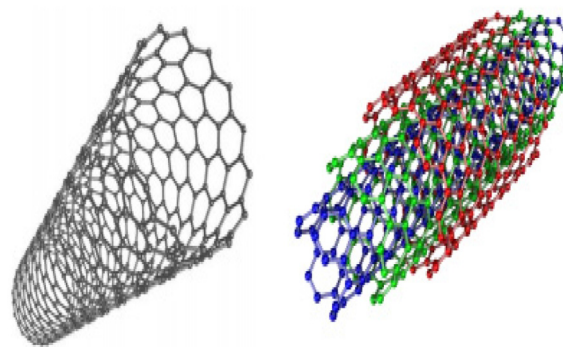chair arrangement. The scientists were excited by this discovery because previously, the problem with nanotubes had been the possibility of several structural variations [73,74].

In a research, it was suggested that the nanotube rope models might not be as homogeneous as initially believed [77]. However, the synthesis of these ropes provided a significant boost to nanotube research.

3.5. MWNT assemblies

Nanotubes produced using the traditional arc method always consist of at least two concentric layers (as shown in Fig. 8), which raises questions about the structural relationship between successive layers [78,79]. Zhang and colleagues [66], as well as Reznik [80], have both examined this issue and arrived at similar conclusions. It has been proposed that the layers of graphene tubes in nanotubes are not cylindrical but instead concentric. Experimental findings suggest that this is likely true for most of CNTs. If there is a distance of approximately 0.334 nm between the concentric graphene tubes, then successive tubes should differ in circumference by $2\pi \times 0.334$ nm or ~2.1 nm. However, this is not possible for zigzag tube structures because 2.1 nm is not a multiple of the actual width of a single hexagon, which is 0.246 nm. The closest approximation to the actual gap is achieved if two consecutive cylinders differ by nine rows of hexagonal ends, resulting in a gap of about 0.352 nm. The bold lines in the figure indicate the nine and eighteen extra rows of atoms added to the middle and outer tubes, respectively. The inclusion of these extra rows is similar to the introduction of a Shockley partial dislocation. The situation is more complex for chiral nanotubes, as it is unlikely that two tubes with precisely the same chiral angle would have a similar gap to a graphite interplanar gap.

3.6. Applications of CNTs

The potential applications of carbon nanotubes and fullerenes are vast, offering a highly diverse technology portfolio. One area of interest is the development of macro-scale devices, where millions or billions of nanotube molecules could be grouped to form lightweight, sturdy wires or compounds suitable for use in vehicles for space and terrestrial applications. The low cost of production could also make it feasible to use these materials in the construction of bridges or for earthquake-resistant building construction. Additionally, they could be used in the production of ammunition and protective vests. CNTs have unique electrical properties that make them ideal for use in smaller and faster computing technologies.

Furthermore, coupling mechanical stimuli with conductivity could make nanotubes valuable in future sub-micro-electromechanical systems. As a result, researchers have recently developed the fullerene amplifier [81]. The main hindrance to achieving better performance of devices based on CNTs and fullerenes is their mechanical fragility. However, CNTs have the potential to be utilized as electron guns for illuminating phosphor coatings on flat-panel screens.

Furthermore, the incorporation of CNTs, graphene, nanoplatelets (GNP), and nano-silica (N.S) as nano-fillers in high-performance composite coatings have demonstrated significant improvements in both the mechanical and electrochemical properties of materials. These coatings have been shown to possess high abrasion resistance, enhanced corrosion resistance, and increased wear resistance, making them suitable for various industrial applications [82,83]. In addition, these materials also have applications in aerospace, automotive, and marine industries [84–87]. The high thermal and electrical conductivity of these nanocomposite coatings makes them suitable for various electronic and energy storage applications. In addition, trapping a fullerene structure inside a CNT of appropriate diameter allows it to move freely between the ends, weakly held per end-cap by van der Waals forces. As a result, an externally applied voltage can drift it from side to side, allowing one bit to be written or read. Therefore, C60 and CNT-based devices can be used as RAM storage in computers.

4. Graphene (2D-Graphite)

The film made of single-layer carbon atoms is arranged in a tightly packed 2-D honeycomb structure, as shown in Fig. 9. This structure can be folded into 0-D fullerenes or rolled to form 1-D nanotubes. Alternatively, the sheets of atoms can be stacked to produce 3-D graphite. Scientists have studied graphene for over 60 years, and it remains the foundation of numerous carbon-based materials developed to date [88]. Despite being a crucial component of three-dimensional materials, graphene was previously believed to be incapable of existing in a free form. It was considered an unstable material compared to its curved counterparts, such as soot, nanotubes, and fullerenes [89].

The experimental confirmation indicated that the charge carrier in graphene was Dirac fermions, which have no mass. This discovery marked a significant breakthrough for this remarkable 2-D material. Additionally, by examining the electronic structure, we can observe rapid changes with the addition of more sheets of an atom. Fig. 10 displays the graphene and its double-layer Raman spectrum. A fermion in graphene behaves as a massless particle, and graphene acts as a zero band gap semiconductor [91]. As the number of layers increases to three or more, the spectrum becomes progressively more complex due to the overlapping of the conduction and valence bands. This results in the charge carriers being trapped in the material [92]. Stacking ten sheets of graphene leads to the formation of the 3-D structure of graphite. This description is consistent with experimental observations.

Even for very thin films, with as little as five layers, it is important to distinguish between the surface and the bulk for the small interlayer distance of approximately 5 Å (less than the thickness of two layers).

In the past, attempts to isolate graphene using chemical treatments [95–97]. Graphite was initially used to separate graphene layers by inserting it
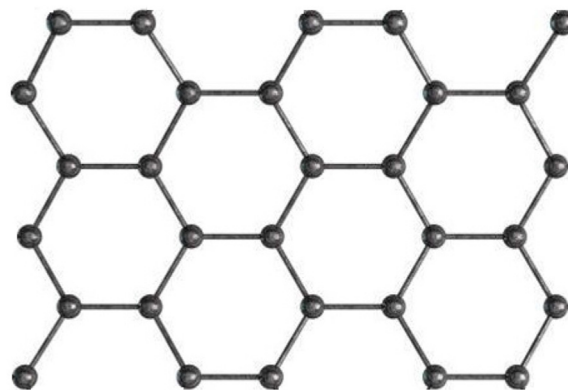

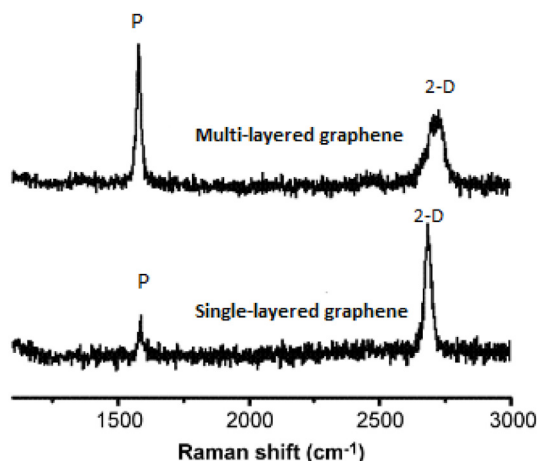*Fig. 9. Graphene hexagonal structure [90].*

Fig. 10. Raman shift spectrum of graphene; P shows intensity peaks obtained in 2-D single-layer graphene are much higher as compared to multilayer assembly [93,94].

between sheets of a crystal, causing layers of superseding atoms to unglue graphene layers. This process often resulted in the formation of new 3-D materials. Another approach involved chemically removing the inserted molecules to obtain a slime of stacked and rolled-up graphene sheets. Several methods were used to separate graphene sheets, including those used for growing CNTs; such attempts were unsuccessful, and only thick graphite flakes of about 100 sheets thick were obtained by this method.

As an alternative, one to a few graphene sheets were created through the CVD (chemical vapour deposition) of hydrocarbons embedded on a metal surface, followed by heating and decomposing SiC [98,99]. The products obtained through these methods were examined using surface science techniques, but their durability and practical application remain unknown. However, using SiC as a substrate, a few graphene layers were found to have remarkable electronic properties and ion mobility [100,101].

The epitaxial approach is currently considered the most feasible for industrial applications [102], and rapid progress is expected in this field. Epitaxial growth on catalytic surfaces may also be a promising avenue for exploration. The process involves depositing an insulating layer on the surface of graphene while removing the platform for metallic growth. However, this method requires further exploration and development.

4.1. Production of graphene

High-quality graphene sheets are challenging to produce; thereby, many experimental researchers are currently using models created by using a method called graphite scotch-taping [103]. This method enabled the isolation of graphene as an initial step and subsequent modifications have facilitated the production of high-quality graphene crystallites of approximately 100 μm in size [104]. At first glance, the technique appears no more sophisticated than drawing with a piece of graphite; however, it involves repeatedly peeling off layers with scotch tape until the thinnest chips are obtained [105]. The challenge in this method is that the crystallites on the substrate are highly irregular and scattered, similar to finding a needle in an ocean. Even with modern techniques for studying graphene, intentionally searching for those small crystallites spread over a 1 cm^2 area would be impossible.

4.2. Electronic structure of graphene

The carbon atoms in graphene are arranged in a hexagonal lattice structure which forms a honeycomb pattern [106,107]. Each unit cell of graphene contains two atoms forming a triangular lattice with lattice vectors:

$$a_1 = \frac{a}{2} \left(3, \sqrt{3}\right).$$

$$a_2 = \frac{a}{2} \left(3, \sqrt{3}\right). \tag{1}$$

Here, a ≈ 1.42 Å, thus:

$$b_1 = \frac{2\pi}{3a} \left(1, \sqrt{3}\right),$$

$$b_2 = \frac{2\pi}{3a} \left(1, -\sqrt{3}\right). \tag{2}$$

The honeycomb structure of graphene results in two conical points in a single Brillouin zone denoted as K and K'. These points are the locations where band crossing occurs. The electron energy depends linearly on the wave vector near these points. This behaviour stems from symmetry assumptions and is robust with respect to long-range hopping processes, as shown in Fig. 11. The spectrum of graphene nearly resembles the Dirac massless fermionic scheme [108].

The Dirac equation describes relativistic quantum particles with a spin of ½, such as electrons. One essential feature of the Dirac spectrum is the existence of antiparticles. In essence, it includes states of both positive and negative energies, which are closely related and described by different components of the same spinor wave function. The
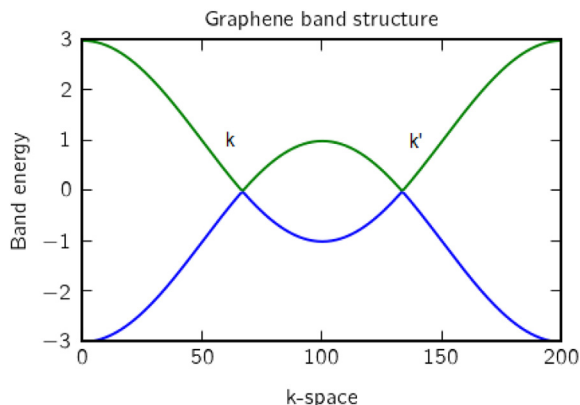
Fig. 11. Graphene band structure [109].

Fig. 12. Arrangement of graphene representing two carbon sub-meshes [112].

property of the aforementioned equation is commonly referred to as charge conjugation symmetryDirac particles with a mass m have a gap between the minimum e−energy, $E_0 = mc^2$, and the max e^+ energy, $-E_0$. If E >> E_0, there is a direct relationship between energy and wave vector, i.e. E = chk. In the case of zero-mass Dirac fermions, the gap is zero, suggesting the linear dispersion relation can be applied to all energy values. In this scenario, there is a close correlation between spin and motion, where the spin can be aligned or opposite to the direction of propagation, with the former case applying to particles and the latter to antiparticles.

On the other hand, massive spin −1/2 particles can exhibit both spin orientations for any direction. However, there is a possibility of particles that are both massless and charged, although there is no substantial evidence to support their existence.

The unique atomic structure of graphene results in its charge carriers being described by a Dirac spectrum instead of the non-relativistic Schrödinger equation typically used for other materials [110]. Graphene consists of two similar carbon sub-meshes, A and B (Fig. 12), and quantum hopping within these sub-meshes produces two energy bands that intersect near the edge of the Brillouin zone, leading to a conical energy spectrum. As a result, quasi-particles within the graphene exhibit a linear dispersion relation given by E = hkμF and appear to have no mass (similar to photons), with Fermi velocity μF approximately equal to c/300. Due to this linear spectrum, quasi-particles in graphene behave differently from traditional metals and semiconductors [111], which have a spectrum that can be approximated using a parabolic dispersion expression. The exceptional electron mobility of graphene has made it possible to observe the elusive Quantum Hall Effect (QHT) at an unprecedented rate.
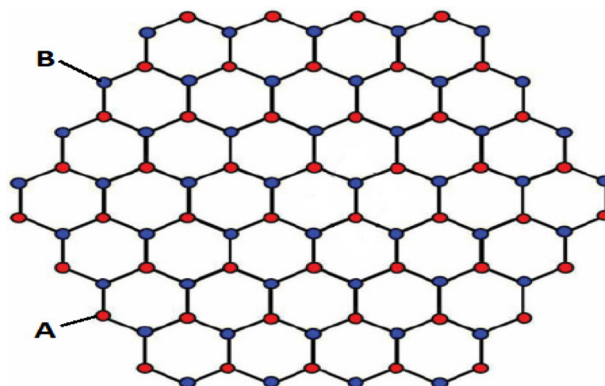
The high mobilities in graphene make it highly responsive to field effects [91]. Consequently, graphene can be considered a compelling alternative to carbon nanotubes (CNTs) for fabricating field-effect transistors (FETs). Additionally, the mobility of graphene is independent of temperature in the range of 10−100 K, suggesting that the primary scattering mechanism is related to the defects in the graphene material.

Through better model preparation, including post-fabrication techniques and current annealing, the mobility of graphene can be increased to greater than 2.5 × 104 cm2/V.s. For oxide-mixed graphene devices, the central scattering elements are confined ions, while for devices on a substrate, the optical phonons of the substrate at room temperatures can enable mobility to reach around 4.0 × 104 cm2/V.s.

Additionally, to enhance mobility, we need to work on better screening procedures [113] or, in some cases, remove the substrate [114]. Through suspension and annealing processes, the equipment can achieve greater mobility, reaching around 2.0 × 10^5 cm^2/V.s. By utilizing suspension and annealing processes, the equipment can achieve greater mobility, reaching around 2.0 × 10^5 cm^2/V.s. Furthermore, experimentally determined conductance shows that the mobility values for positive and negative ions are approximately the same.

The description of graphene can be given by the minimum conductance value, often represented as e^2/h [115,116]. This is the highest mobility value obtained so far for a semiconductor. Moreover, the mobility remains high even at high electric field-created charge densities and appears slightly perturbed by chemical doping. This suggests the possibility of achieving a ballistic transport system on a sub-micrometre scale at a temperature of around 300K. Additionally, experimentally determined

conductance shows that the mobility values for positive and negative ions are approximately the same. The mean free path, λ, can be assessed from the results obtained by conductivity experiments. Before and after annealing, the mean free path, λ, increases from 150 nm to 1 μm, and the latter distance is nearly equal to, but not less than, the size of nanoscale devices. The ion transport in this device that affects ion conduction is non-diffusive and approaches the ballistic limit.

Another unique aspect of the electronic characteristics is the strictly linear dispersion curve around the Dirac point, which leads to the consecutive observation of the Berry phase or a quantum Hall effect, as mentioned earlier [66]. This results in K and $\acute{K}$ valleys and pseudospin degeneracy. Similarly, bilayer graphene exhibits a different behaviour due to the absence of a gap in the parabolic dispersion, resulting in the availability of two additional bands.

In addition to the above-stated property of a large electronic coherence distance, the spin coherence length is also of significance, with a value of approximately one μm, which allows for the fabrication of spintronic devices. The linear dispersion graph with a vanishing density of states at the node point of the valence and conduction bands precludes nonlinear attributes. Field-effect-induced modulation of transport features is ineffective in graphene. Apart from FETs, this has spurred the search for electronic gap properties of graphene, aiming to use it in various electrical applications such as energy storage devices [117].

4.3. Applications in sensor and manufacturing nanocomposites

A sensor is a sophisticated tool that involves integrating various features, ranging from user-friendliness to conversion efficiency. It necessitates molecular-level sensitivity, as well as mechanical and electrical expertise. Graphene satisfies most of these demands, and the development of highly sensitive graphene sensors could demonstrate how the aforementioned characteristics can be achieved to accomplish specific tasks [118]. Undoubtedly, suspended graphene provides a clean interface with all atoms exposed to the surrounding environment. It is chemically stable and can be functional in some form of interaction.

Moreover, the confined destruction of the sp^2 matrix preserves its mechanical strength and does not compromise its 2D transport properties, unlike carbon nanotubes (CNTs). The electronic and mechanical behaviour can be manipulated to achieve the transduction of the sensing signal. Lastly, graphene and its oxidized forms are more cost-effective compared to other graphite-based materials like CNTs. Currently, it is being considered for sensing phases. In the gas molecule adsorption phase on the graphene surface, the local change in carrier densities involves doping the delocalized 2D-EG [119,120], which can be observed electrically in a transistor-based arrangement.

Contrary to other materials, the extraordinary mobility, area contact, and ability for good conductivity [121], graphene underwrite to confine the background noise in transport research. This makes graphene FET devices highly sensitive and capable of detecting particles as low as parts per billion and at a surprisingly rapid rate, as demonstrated in experiments. However, the sensitivity of processed graphene (i.e. remaining resist after lithography) is significantly offset. Therefore, the functionalization of graphene oxide is desirable to enhance its sensitivity. Graphene sensitivity is not restricted to chemical phenomena but can be applied to any phenomenon that causes a local change in carrier density, such as a magnetic field, deformation from mechanical processes, or external ions. Another approach to electrical detection is to leverage the electro-mechanical properties of suspended graphene, similar to non-mechanical CNT sensors, which can achieve sensitivities down to the level of a single atom [122]. The large surface area and stiffness of such graphene make it suitable for use as mechanical mass sensors, as evidenced by its Raman signature.

Apart from the sensor, graphene-based high-performance composite coatings are being developed by incorporating nanoparticles in the polymer resins. These coatings are being tested in manufacturing material for oil and gas pipelines [123], where large agglomeration observed at the higher concentrations mainly resulted in reduced corrosion and abrasion resistance. On the other hand, nano-modified functional composite coatings for metallic structures suggested that a 0.5–1.5 wt% of nanofiller can improve mechanical and electrochemical properties [72].

In addition, a later study showed that the nanocomposites reinforced by different nanoparticles exhibited improved Young's modulus, tensile strength, and ultimate strain [83]. Moreover, such nanocomposites, including metallic and epoxy coatings, have potential applications with anticorrosion, self-cleaning and antiwear properties and can be used effectively in the construction industry [124–126].

5. Limitations of carbon allotropes

Carbon allotropes are highly promising materials for various applications, but several limitations must be addressed before their full potential can be realised. Some of these limitations include the following.

- The chirality of a CNT determines its electronic and mechanical properties, and it can be challenging to control during the synthesis process. As a result, the properties of CNTs can vary significantly, and it can be challenging to produce CNTs with consistent properties.
- While significant progress has been made in synthesising CNTs, scalability and cost-effectiveness are still limitations. Current methods for producing CNTs are energy-intensive, require expensive equipment, and can create a low yield of high-quality CNTs.
- Structural defects, such as vacancies, can occur during the synthesis of CNTs, which can affect their electronic and mechanical properties. The presence of defects can also decrease the strength and stability of CNTs.
- CNTs are relatively inert and have limited functionalization, which can limit their potential applications. The functionalization of CNTs can enhance their properties, such as solubility, reactivity, and selectivity, and enable new applications.
- Single-walled CNTs (SWCNTs) are highly desired due to their unique properties, but they are challenging to produce in large quantities. SWCNTs are typically grown as a mixture of different chiralities, and separating and purifying them can be challenging.
- The graphene has a zero band gap, which causes difficulty in manufacturing on a large scale and sensitivity to impurities which can affect its properties and performance.
- Graphene is also very fragile, making it challenging to handle and integrate into devices. And the relative cost of manufacturing high-quality graphene is still relatively high, which limits its use in some commercial applications.

Apart from these limitations, future research can focus on developing new methods for synthesising and functionalised CNTs, understanding their properties and potential applications, and addressing their limitations.

6. Summary and conclusion

Thus far, we have explored the structures and notable characteristics of various carbon nano-assemblies, including fullerenes, carbon nanotubes (CNTs), and graphene. Fullerenes and their derivatives exhibit exceptional superconducting behaviour and have potential applications in a variety of fields. Spectroscopic methods have also revealed the presence of distinct long and short bonds between hexagonal and pentagonal rings in fullerenes. The straining of these bonds gives fullerene its characteristic caged structure. The addition of CH_2N_2 byproduct has produced structures such as fulleroids and methanol-fullerene, which can be used as thin film coating materials with high optical qualities in polymers. One of the essential techniques is the electric arc method, which is commonly used to synthesize CNTs. There are challenges such as defect, scalability and production cost, which produce low yields of good quality CNTs and limitations to the effective use of CNTs. The zero band gap of graphene presents challenges in large-scale manufacturing, and its sensitivity to impurities can significantly impact its properties and performance. In addition, all the carbon allotropes, including graphene, can be effectively used to construct high-performance nanocomposites, enhancing various physical, optical and thermal properties of materials.

Acknowledgements

Conflict of interest

The authors declare no conflict of interest

References

[1] M. Saeed, W. Uddin, A.S. Saleemi, M. Hafeez, M. Kamil, I.A. Mir, Sunila, R. Ullah, S.U. Rehman, Z. Ling, Optoelectronic properties of MoS2-ReS2 and ReS2-MoS2 heterostructures, Phys. B Condens. Matter 577 (2020) 411809, https://doi.org/10.1016/j.physb.2019.411809.

[2] S. Talebi, M. Sadighi, Simulation of compression behavior of porous structure based on different space-filling unit cells under quasi-static loading, Mech. Base. Des. Struct. Mach. (2021) 1–15, https://doi.org/10.1080/15397734.2021.1903492.

[3] L. Pauling, R.B. Corey, Configurations of polypeptide chains with favored orientations around single bonds: two new pleated sheets, Proc. Natl. Acad. Sci. U. S. A 37 (1951) 729–740, https://doi.org/10.1073/pnas.37.11.729.

[4] M. Ross, A.M. Langer, G.L. Nord, R.P. Nolan, R.J. Lee, D. Van Orden, J. Addison, The mineral nature of asbestos, Regul. Toxicol. Pharmacol. 52 (2008), https://doi.org/10.1016/j.yrtph.2007.09.008. S26–S30.

[5] T. Abdullahi, Z. Harun, M.H.D. Othman, A review on sustainable synthesis of zeolite from kaolinite resources via hydrothermal process, Adv. Powder Technol. 28 (2017) 1827–1840, https://doi.org/10.1016/j.apt.2017.04.028.

[6] W.N. Lipscomb, The boranes and their relatives, Science 196 (1977) 1047–1055, https://doi.org/10.1126/science.196.4294.1047.

[7] J.A. Pople, D.L. Beveridge, P.A. Dobosh, Approximate self-consistent molecular-orbital theory. V. Intermediate neglect of differential overlap, J. Chem. Phys. 47 (1967) 2026–2033, https://doi.org/10.1063/1.1712233.

[8] A. Arshad, M. Jabbal, Y. Yan, D. Reay, A review on graphene based nanofluids: preparation, characterization and applications, J. Mol. Liq. 279 (2019) 444–484, https://doi.org/10.1016/j.molliq.2019.01.153.

[9] W. Choi, I. Lahiri, R. Seelaboyina, Y.S. Kang, Synthesis of graphene and its applications: a review, Crit. Rev. Solid State Mater. Sci. 35 (2010) 52–71, https://doi.org/10.1080/10408430903505036.

[10] M.I. Katsnelson, Graphene: carbon in two dimensions, Mater. Today 10 (2007) 20–27, https://doi.org/10.1016/S1369-7021(06)71788-6.

[11] Z. Shen, W. Li, J. Ma, X. Zhang, X. Zhang, X. Zhang, P. Dong, S. Wang, J. Xu, X. Zhang, Theoretical predictions of size-dependent Young's and shear moduli of single-walled carbon nanotubes, Phys. B Condens. Matter 613 (2021) 412994, https://doi.org/10.1016/j.physb.2021.412994.

[12] S. Ajori, S.H. Boroushak, R. Hassani, R. Ansari, A molecular dynamics study on the buckling behavior of x-graphyne based single- and multi-walled nanotubes, Comput. Mater. Sci. 191 (2021) 110333, https://doi.org/10.1016/j.commatsci.2021.110333.

[13] W. Chang, F. Liu, Y. Liu, T. Zhu, L. Fang, Q. Li, Y. Liu, X. Zhao, Smallest carbon nanowires made easy: long linear carbon chains confined inside single-walled carbon nanotubes, Carbon N. Y. 183 (2021) 571–577, https://doi.org/10.1016/j.carbon.2021.07.037.

[14] M. Karimi, Investigation of behavior and analysis of mechanical properties of carbon nanotubes under different loads, J. Chem. Rev. 3 (2021) 134–146, https://doi.org/10.22034/jcr.2021.285154.1110.

[15] S. Kamarian, M. Bodaghi, R.B. Isfahani, M. Shakeri, M.H. Yas, Influence of carbon nanotubes on thermal expansion coefficient and thermal buckling of polymer composite plates: experimental and numerical investigations, Mech. Base. Des. Struct. Mach. 49 (2021) 217–232, https://doi.org/10.1080/15397734.2019.1674664.

[16] A. Hashimoto, K. Suenaga, A. Gloter, K. Urita, S. Iijima, Direct evidence for atomic defects in graphene layers, Nature 430 (2004) 870–873, https://doi.org/10.1038/nature02817.

[17] J. Low, S. Cao, J. Yu, S. Wageh, Two-dimensional layered composite photocatalysts, Chem. Commun. 50 (2014) 10768, https://doi.org/10.1039/C4CC02553A.

[18] A.C. Ferrari, J. Robertson, Interpretation of Raman spectra of disordered and amorphous carbon, Phys. Rev. B 61 (2000) 14095–14107, https://doi.org/10.1103/PhysRevB.61.14095.

[19] S. Bakhsh, X. Liu, Y. Wang, L. He, X. Ren, Beryllium and magnesium metal clusters: new globally stable structures and G 0 W 0 calculations, J. Phys. Chem. 125 (2021) 1424–1435, https://doi.org/10.1021/acs.jpca.0c08960.

[20] C. García-Simón, M. Garcia-Borràs, L. Gómez, T. Parella, S. Osuna, J. Juanhuix, I. Imaz, D. Maspoch, M. Costas, X. Ribas, Sponge-like molecular cage for purification of fullerenes, Nat. Commun. 5 (2014) 5557, https://doi.org/10.1038/ncomms6557.

[21] H.W. Kroto, The stability of the fullerenes Cn, with n = 24,28,32,36,50,60 and 70, Nature 329 (1987) 529–531, https://doi.org/10.1038/329529a0.

[22] S. Iijima, Nature publishing group, Nature 354 (1991) 56–58, https://doi.org/10.1038/354056a0.

[23] R.E. Smalley, Discovering the fullerenes(nobel lecture), Angew Chem. Int. Ed. Engl. 36 (1997) 1594–1601, https://doi.org/10.1002/anie.199715941.

[24] R.C. Haddon, Chemistry of the fullerenes: the manifestation of strain in a class of continuous aromatic molecules, Science 261 (1993) 1545–1550, https://doi.org/10.1126/science.261.5128.1545.

[25] W. Yu, H. Xie, A review on nanofluids: preparation, stability mechanisms, and applications, J. Nanomater. 2012 (2012) 1–17, https://doi.org/10.1155/2012/435873.

[26] S. Dastjerdi, B. Akgöz, On the statics of fullerene structures, Int. J. Eng. Sci. 142 (2019) 125–144, https://doi.org/10.1016/j.ijengsci.2019.06.002.

[27] M. Prato, Fullerene chemistry for materials science applications, J. Mater. Chem. 7 (1997) 1097–1109, https://doi.org/10.1039/a700080d.

[28] K. Lee, H. Song, J.T. Park, Fullerene-metal cluster complexes: novel bonding modes and electronic communication, Acc. Chem. Res. 36 (2003) 78–86, https://doi.org/10.1021/ar020149a.

[29] T.C. Dinadayalane, J. Leszczynski, Chapter 7 toward nanomaterials: structural, energetic and reactivity aspects of single-walled carbon nanotubes, in: Theor. Comput. Chem., Elsevier. 2007, pp. 167–199, https://doi.org/10.1016/S1380-7323(06)80009-9.

[30] Z. Chen, W. Thie, A. Hirsch, Reactivity of the Convex and Concave Surfaces of Single-Walled Carbon Nanotubes (SWCNTs) towards Addition Reactions Dependence on the Carbon.Pdf, vol. 4, Wiley Online Libr. 2003, pp. 93–97, https://doi.org/10.1002/cphc.200390015.

[31] L.S. Porto, D.N. Silva, A.E.F. de Oliveira, A.C. Pereira, K.B. Borges, Carbon nanomaterials: synthesis and applications to development of electrochemical sensors in determination of drugs and compounds of clinical interest, Rev. Anal. Chem. 38 (2020) 20190017, https://doi.org/10.1515/revac-2019-0017.

[32] F. Diederich, L. Isaacs, D. Philp, Syntheses , structures, and properties of methanofullerenes, Chem. Soc. Rev. 23 (1994) 243–255, https://doi.org/10.1039/CS9942300243.

[33] T. Suzuki, Q. Li, K.C. Khemani, F. Wudl, Dihydrofulleroid H3C61: synthesis and properties of the parent fulleroid, J. Am. Chem. Soc. 114 (1992) 7301–7302, https://doi.org/10.1021/ja00044a055.

[34] M. Prato, V. Lucchini, M. Maggini, E. Stimpfl, G. Scorrano, M. Eiermann, T. Suzuki, F. Wudl, Energetic preference in 5,6 and 6,6 ring junction adducts of C60: fulleroids and methanofullerenes, J. Am. Chem. Soc. 115 (1993) 8479–8480, https://doi.org/10.1021/ja00071a080.

[35] H.O. Pierson, Graphite structure and properties, in: Handb. Carbon, Graph. Diamonds Fullerenes, Elsevier. 1993, pp. 43–69, https://doi.org/10.1016/B978-0-8155-1339-1.50008-6.

[36] J.N. Coleman, U. Khan, Y.K. Gun'ko, Mechanical reinforcement of polymers using carbon nanotubes, Adv. Mater. 18 (2006) 689–706, https://doi.org/10.1002/adma.200501851.

[37] C.J. Frizzell, D.H. Coutinho, K.J. Balkus, A.I. Minett, W.J. Blau, J.N. Coleman, Phys. Rev. B 72 (2005) 245420, https://doi.org/10.1103/PhysRevB.72.245420.

[38] Y.A. Iijima, Preparation of carbon nanotubes by arc-discharge evaporation, Jpn. J. Appl. Phys. 32 (1993) L107, https://doi.org/10.1143/JJAP.32.L107.

[39] V. Choudhary, B.P. Singh, R.B. Mathur, Carbon nanotubes and their composites, Synth. Appl. Carbon Nanotube. Their Compos. (2013) 193–222, https://doi.org/10.5772/3377.

[40] C.T. Kingston, B. Simard, Fabrication of carbon nanotubes, Anal. Lett. 36 (2003) 3119–3145, https://doi.org/10.1081/AL-120026564.

[41] K. Kobashi, S. Ata, T. Yamada, D.N. Futaba, T. Okazaki, K. Hata, Classification of commercialized carbon nanotubes into three general categories as a guide for applications, ACS Appl. Nano Mater. 2 (2019) 4043–4047, https://doi.org/10.1021/acsanm.9b00941.

[42] M.S. Dresselhaus, Science of fullerenes and carbon nanotubes, in: Sci. Fullerenes Carbon Nanotub., first ed., Academic Press. 1996, pp. 60–792, https://doi.org/10.1016/b978-0-12-221820-0.x5000-x.

[43] P.G. Collins, K. Bradley, M. Ishigami, A. Zettl, Extreme oxygen sensitivity of electronic properties of carbon

nanotubes, Science (80) 287 (2000) 1801–1804, https://doi.org/10.1126/science.287.5459.1801.

[44] H.W. Kroto, J.E. Fischer, D. Cox, The Fullerenes, first ed., Elsevier. 1993, pp. 2–5, https://doi.org/10.1016/C2009-0-11235-7.

[45] R. Bacon, Growth, structure, and properties of graphite whiskers, J. Appl. Phys. 31 (1960) 283–290, https://doi.org/10.1063/1.1735559.

[46] B.I. Yakobson, R.E. Smalley, Fullerene Nanotubes: C 1,000,000 and Beyond: some unusual new molecules—long, hollow fibers with tantalizing electronic and mechanical properties—have joined diamonds and graphite in the carbon family, Am. Sci. 85 (1997) 324–337, https://doi.org/10.2307/27856810.

[47] P.M. Ajayan, T.W. Ebbesen, T. Ichihashi, S. Iijima, K. Tanigaki, H. Hiura, Opening carbon nanotubes with oxygen and implications for filling, Nature 362 (1993) 522–525, https://doi.org/10.1038/362522a0.

[48] T. Guo, P. Nikolaev, A. Thess, D.T. Colbert, R.E. Smalley, Catalytic growth of single-walled nanotubes by laser vaporization, Chem. Phys. Lett. 243 (1995) 49–54, https://doi.org/10.1016/0009-2614(95)00825-O.

[49] K.R. Bates, G.E. Scuseria, Energetic analysis of pentagon road intermediates of C-60-buckminsterfullerene formation, J. Phys. Chem. 101 (1997) 3038–3041, https://doi.org/10.1021/jp964021k.

[50] K.S. Ibrahim, Carbon nanotubes-properties and applications: a review, Carbon Lett 14 (2013) 131–144, https://doi.org/10.5714/CL.2013.14.3.131.

[51] R. Saito, M. Fujita, G. Dresselhaus, M.S. Dresselhaus, Electronic structure of chiral graphene tubules, Appl. Phys. Lett. 60 (1992) 2204–2206, https://doi.org/10.1063/1.107080.

[52] a V. Krasheninnikov, F. Banhart, Engineering of nanostructured carbon materials with electron or ion beams, Nat. Mater. 6 (2007) 723–733, https://doi.org/10.1038/nmat1996.

[53] A. Pantano, D.M. Parks, M.C. Boyce, Mechanics of deformation of single- and multi-wall carbon nanotubes, J. Mech. Phys. Solid. 52 (2004) 789–821, https://doi.org/10.1016/j.jmps.2003.08.004.

[54] L.A. Girifalco, M. Hodak, R.S. Lee, Carbon nanotubes, buckyballs, ropes, and a universal graphitic potential, Phys. Rev. B 62 (2000) 13104–13110, https://doi.org/10.1103/PhysRevB.62.13104.

[55] E. Hernández, C. Goze, P. Bernier, A. Rubio, Elastic properties of single-wall nanotubes, Appl. Phys. Mater. Sci. Process 68 (1999) 287–292, https://doi.org/10.1007/s003390050890.

[56] A. Thess, R. Lee, P. Nikolaev, H. Dai, P. Petit, J. Robert, C. Xu, Y.H. Lee, S.G. Kim, A.G. Rinzler, D.T. Colbert, G.E. Scuseria, D. Tomanek, J.E. Fischer, R.E. Smalley, Crystalline ropes of metallic carbon nanotubes, Science (80) 273 (1996) 483–487, https://doi.org/10.1126/science.273.5274.483.

[57] E.T. Thostenson, Z. Ren, T.-W. Chou, Advances in the science and technology of carbon nanotubes and their composites: a review, Compos. Sci. Technol. 61 (2001) 1899–1912, https://doi.org/10.1016/S0266-3538(01)00094-X.

[58] T. Brintlinger, M.S. Fuhrer, J. Melngailis, I. Utke, T. Bret, A. Perentes, P. Hoffmann, M. Abourida, P. Doppelt, Electrodes for carbon nanotube devices by focused electron beam induced deposition of gold, J. Vac. Sci. Technol. B Microelectron. Nanom. Struct. 23 (2005) 3174, https://doi.org/10.1116/1.2130355.

[59] C. Dekker, Carbon nanotubes as molecular quantum wires, Phys. Today 52 (1999) 22–28, https://doi.org/10.1063/1.882658.

[60] C. Lieber, T. Rueckes, E. Joselevich, K. Kim, Nanoscopic Wire-Based Devices, Arrays, and Methods of Their Manufacture, US20020130353A1. 2001.

[61] E. Stern, A. Nanowire, Methods for Fabricating Ohmic Contacts to Nanowires and Nanotubes, 2006, pp. 231–236, https://doi.org/10.1116/1.2162575.

[62] A. Bachtold, M. Henny, C. Terrier, C. Strunk, C. Schönenberger, J.P. Salvetat, J.M. Bonard, L. Forró, Contacting carbon nanotubes selectively with low-ohmic contacts for four-probe electric measurements, Appl. Phys. Lett. 73 (1998) 274–276, https://doi.org/10.1063/1.121778.

[63] H. Dai, Carbon nanotubes: synthesis, integration, and properties, Acc. Chem. Res. 35 (2002) 1035–1044, https://doi.org/10.1021/ar0101640.

[64] V.V. Pokropivnyi, Non-carbon nanotubes (review). III. Properties and applications, Powder Metall. Met. Ceram. 41 (2002) 123–135, https://doi.org/10.1023/A:1019874624638.

[65] H. Shima, Buckling of carbon nanotubes: a state of the art review, Materials 5 (2012) 47–84, https://doi.org/10.3390/ma5010047.

[66] G. Zhang, B. Li, Thermal conductivity of nanotubes revisited: effects of chirality, isotope impurity, tube length, and temperature, J. Chem. Phys. 123 (2005) 114714, https://doi.org/10.1063/1.2036967.

[67] P. Avouris, T. Hertel, R. Martel, T. Schmidt, H.R. Shea, R.E. Walkup, Carbon nanotubes: nanomechanics, manipulation, and electronic devices, Appl. Surf. Sci. 141 (1999) 201–209, https://doi.org/10.1016/S0169-4332(98)00506-6.

[68] R. Baughman, A. Zakhidov, W. de Heer, Carbon NanotubesOThe route toward applications, Science (80) 297 (2002) 787–792, https://doi.org/10.1126/science.1060928.

[69] S. Iijima, T. Ichihashi, Single-shell carbon nanotubes of 1-nm diameter, Nature 363 (1993) 603–605, https://doi.org/10.1038/363603a0.

[70] A. Cao, C. Xu, J. Liang, D. Wu, B. Wei, X-ray diffraction characterization on the alignment degree of carbon nanotubes, Chem. Phys. Lett. 344 (2001) 13–17, https://doi.org/10.1016/S0009-2614(01)00671-6.

[71] P.J.F. Harris, E. Hernández, B.I. Yakobson, Carbon nanotubes and related structures: new materials for the twenty-first century, Am. J. Phys. 72 (2004), https://doi.org/10.1119/1.1645289, 415–415.

[72] K.B. Shelimov, R.O. Esenaliev, A.G. Rinzler, C.B. Huffman, R.E. Smalley, Purification of single-wall carbon nanotubes by ultrasonically assisted filtration, Chem. Phys. Lett. 282 (1998) 429–434, https://doi.org/10.1016/S0009-2614(97)01265-7.

[73] J. Liu, A.G. Rinzler, H. Dai, J.H. Hafner, R.K. Bradley, P.J. Boul, A. Lu, T. Iverson, K. Shelimov, C.B. Huffman, F. Rodriguez-Macias, Y.-S. Shon, T.R. Lee, D.T. Colbert, R.E. Smalley, Fullerene pipes, Science 280 (1998) 1253–1256, https://doi.org/10.1126/science.280.5367.1253.

[74] S.J. Tans, M.H. Devoret, H. Dai, A. Thess, R.E. Smalley, L.J. Geerligs, C. Dekker, Individual single-wall carbon nanotubes as quantum wires, Nature 386 (1997) 474–477, https://doi.org/10.1038/386474a0.

[75] Y. Zhang, Y. Bai, B. Yan, Functionalized carbon nanotubes for potential medicinal applications, Drug Discov. Today 15 (2010) 428–435, https://doi.org/10.1016/j.drudis.2010.04.005.

[76] Z.U. Khan, A. Kausar, H. Ullah, A review on composite papers of graphene oxide, carbon nanotube, polymer/GO, and polymer/CNT: processing strategies, properties, and relevance, Polym. Plast. Technol. Eng. 55 (2016) 559–581, https://doi.org/10.1080/03602559.2015.1098693.

[77] O. Zhou, H. Shimoda, B. Gao, S. Oh, L. Fleming, G. Yue, Materials science of carbon nanotubes: fabrication, integration, and properties of macroscopic structures of carbon nanotubes, Acc. Chem. Res. 35 (2002) 1045–1053, https://doi.org/10.1021/ar010162f.

[78] F. Khan, A. Kausar, M. Siddiq, A review on properties and fabrication techniques of polymer/carbon nanotube composites and polymer intercalated buckypapers, Polym. Plast. Technol. Eng. 54 (2015) 1524–1539, https://doi.org/10.1080/03602559.2015.1021486.

[79] V. Popov, Carbon nanotubes: properties and application, Mater. Sci. Eng. R Rep. 43 (2004) 61–102, https://doi.org/10.1016/j.mser.2003.10.001.

[80] D. Reznik, C.H. Olk, D.A. Neumann, J.R.D. Copley, X-ray powder diffraction from carbon nanotubes and

nanoparticles, Phys. Rev. B 52 (1995) 116–124, https://doi.org/10.1103/PhysRevB.52.116.

[81] B. Li, X. Cao, H.G. Ong, J.W. Cheah, X. Zhou, Z. Yin, H. Li, J. Wang, F. Boey, W. Huang, H. Zhang, All-carbon electronic devices fabricated by directly grown single-walled carbon nanotubes on reduced graphene oxide electrodes, Adv. Mater. 22 (2010) 3058–3061, https://doi.org/10.1002/adma.201000736.

[82] X. Wang, M. Pearson, H. Pan, M. Li, Z. Zhang, Z. Lin, Nano-modified functional composite coatings for metallic structures: Part I-Electrochemical and barrier behavior, Surf. Coating. Technol. 401 (2020) 126286, https://doi.org/10.1016/j.surfcoat.2020.126286.

[83] X. Wang, F. Tang, Q. Cao, X. Qi, H. Pan, Z. Lin, D. Battocchi, Nano-modified functional composite coatings for metallic structures: Part II—mechanical and damage tolerance, Surf. Coating. Technol. 401 (2020) 126274, https://doi.org/10.1016/j.surfcoat.2020.126274.

[84] X. Wang, F. Tang, Q. Cao, X. Qi, H. Pan, X. Chen, Z. Lin, Carbon-based nanoparticle-filled protective coatings for enhanced damage tolerance and corrosion resistance of structural weldment, J. Mater. Civ. Eng. 34 (2022) 126286, https://doi.org/10.1061/(ASCE)MT.1943-5533.0004019.

[85] X. Wang, Z. Lin, Robust, hydrophobic anti-corrosion coating prepared by PDMS modified epoxy composite with graphite nanoplatelets/nano-silica hybrid nanofillers, Surf. Coating. Technol. 421 (2021) 127440, https://doi.org/10.1016/j.surfcoat.2021.127440.

[86] X. Wang, F. Tang, X. Qi, Z. Lin, D. Battocchi, X. Chen, Enhanced protective coatings based on nanoparticle fullerene C60 for oil & gas pipeline corrosion mitigation, Nanomaterials 9 (2019) 1476, https://doi.org/10.3390/nano9101476.

[87] X. Wang, Z. Lin, Morphologic and synergistic effects of GNP/NS binary-filler-based multifunctional coatings with robust anti-corrosion and hydrophobic properties, Prog. Org. Coating 157 (2021) 106286, https://doi.org/10.1016/j.porgcoat.2021.106286.

[88] S.K. Tiwari, S. Sahoo, N. Wang, A. Huczko, Graphene research and their outputs: status and prospect, J. Sci. Adv. Mater. Devices. 5 (2020) 10–29, https://doi.org/10.1016/j.jsamd.2020.01.006.

[89] K.S. Novoselov, A.K. Geim, S. V Morozov, D. Jiang, M.I. Katsnelson, I. V Grigorieva, S. V Dubonos, A.A. Firsov, Two-dimensional gas of massless Dirac fermions in graphene, Nature 438 (2005) 197–200, https://doi.org/10.1038/nature04233.

[90] R. Rudrapati, Graphene: fabrication methods, properties, and applications in modern industries, in: Graphene Prod. Appl., IntechOpen. 2020, pp. 9–22, https://doi.org/10.5772/intechopen.92258.

[91] S.V. Morozov, K.S. Novoselov, D. Jiang, A.A. Firsov, S.V. Dubonos, A.K. Geim, Two dimensional electron and hole gases at the surface of graphite, Phys. Rev. B Condens. Matter 72 (2005) 201401, https://doi.org/10.1103/PhysRevB.72.201401.

[92] M.F. Craciun, S. Russo, M. Yamamoto, S. Tarucha, Tuneable electronic properties in graphene, Nano Today 6 (2011) 42–60, https://doi.org/10.1016/j.nantod.2010.12.001.

[93] M.A. Pimenta, G. Dresselhaus, M.S. Dresselhaus, L.G. Cançado, A. Jorio, R. Saito, Studying disorder in graphite-based systems by Raman spectroscopy, Phys. Chem. Chem. Phys. 9 (2007) 1276–1291, https://doi.org/10.1039/b613962k.

[94] A.C. Ferrari, J.C. Meyer, V. Scardaci, C. Casiraghi, M. Lazzeri, F. Mauri, S. Piscanec, D. Jiang, K.S. Novoselov, S. Roth, A.K. Geim, Raman spectrum of graphene and graphene layers, Phys. Rev. Lett. 97 (2006) 187401, https://doi.org/10.1103/PhysRevLett.97.187401.

[95] S. Park, R.S. Ruoff, Chemical methods for the production of graphenes, Nat. Nanotechnol. 4 (2009) 217–224, https://doi.org/10.1038/nnano.2009.58.

[96] D.R. Dreyer, S. Park, C.W. Bielawski, R.S. Ruoff, The chemistry of graphene oxideThe chemistry of graphene oxide, Chem. Soc. Rev. 39 (2010) 228–240, https://doi.org/10.1039/b917103g.

[97] A. Reina, X. Jia, J. Ho, D. Nezich, H. Son, V. Bulovic, M.S. Dresselhaus, J. Kong, Large area, few-layer graphene films on arbitrary substrates by chemical vapor deposition, Nano Lett. 9 (2009) 30–35, https://doi.org/10.1021/nl801827v.

[98] S. Tkachev, E. Buslaeva, S. Gubin, Graphene: a novel carbon nanomaterial, Inorg. Mater. 47 (2011) 1–10, https://doi.org/10.1134/s0020168511010134.

[99] W. Zhang, A.C.T. van Duin, Atomistic-scale simulations of the graphene growth on a silicon carbide substrate using thermal decomposition and chemical vapor deposition, Chem. Mater. 32 (2020) 8306–8317, https://doi.org/10.1021/acs.chemmater.0c02121.

[100] K. V Emtsev, F. Speck, T. Seyller, L. Ley, J.D. Riley, Interaction, growth, and ordering of epitaxial graphene on SiC {0001} surfaces: a comparative photoelectron spectroscopy study, Phys. Rev. B Condens. Matter 77 (2008) 1–10, https://doi.org/10.1103/PhysRevB.77.155303.

[101] J. Hass, W. a de Heer, E.H. Conrad, The growth and morphology of epitaxial multilayer graphene, J. Phys. Condens. Matter 20 (2008) 323202, https://doi.org/10.1088/0953-8984/20/32/323202.

[102] M. Sharon, M. Sharon, Graphene, first ed., John Wiley & Sons, Inc., Hoboken, NJ, USA. 2015, pp. 10–12, https://doi.org/10.1002/9781118842577.

[103] A.K. Geim, Graphene: status and prospects, Science 324 (2009) 1530–1534, https://doi.org/10.1126/science.1158877.

[104] A.N. Obraztsov, A.A. Zolotukhin, A.O. Ustinov, A.P. Volkov, Y.P. Svirko, Chemical vapor deposition of carbon films: in-situ plasma diagnostics, Carbon N. Y. 41 (2003) 836–839, https://doi.org/10.1016/S0008-6223(02)00402-5.

[105] V. Singh, D. Joung, L. Zhai, S. Das, S.I. Khondaker, S. Seal, Graphene based materials: past, present and future, Prog. Mater. Sci. 56 (2011) 1178–1271, https://doi.org/10.1016/j.pmatsci.2011.03.003.

[106] F. Schäffel, in: J.H. Warner, F. Schäffel, A. Bachmatiuk, M.H. Rümmeli, eds., The Atomic Structure of Graphene and its Few-Layer Counterparts, Graphene, Elsevier. 2013, pp. 5–59, https://doi.org/10.1016/B978-0-12-394593-8.00002-3.

[107] M.J. Allen, V.C. Tung, R.B. Kaner, Honeycomb carbon: a review of graphene, Chem. Rev. 110 (2010) 132–145, https://doi.org/10.1021/cr900070d.

[108] G.W. Semenoff, Condensed-Matter simulation of a three-Dimensional anomaly, Phys. Rev. Lett. 53 (1984) 2449–2452, https://doi.org/10.1103/PhysRevLett.53.2449.

[109] M.S. Mrudul, G. Dixit, Controlling valley-polarisation in graphene via tailored light pulses, J. Phys. B Atom. Mol. Opt. Phys. 54 (2021) 224001, https://doi.org/10.1088/1361-6455/ac41ae.

[110] K.S. Kim, A.L. Walter, L. Moreschini, T. Seyller, K. Horn, E. Rotenberg, A. Bostwick, Coexisting massive and massless Dirac fermions in symmetry-broken bilayer graphene, Nat. Mater. 12 (2013) 887–892, https://doi.org/10.1038/nmat3717.

[111] A. Bostwick, T. Ohta, T. Seyller, K. Horn, E. Rotenberg, Quasiparticle dynamics in graphene, Nat. Phys. 3 (2007) 36–40, https://doi.org/10.1038/nphys477.

[112] I.O. Raikov, D.A. Conyuh, A.N. Ipatov, D.A. Parshin, A theory of flexural modes in graphene, J. Phys. Conf. Ser. 1695 (2020) 012179, https://doi.org/10.1088/1742-6596/1695/1/012179.

[113] T. Ando, Anomaly of optical phonon in monolayer graphene, J. Phys. Soc. Japan. 75 (2006) 124701, https://doi.org/10.1143/JPSJ.75.124701.

[114] J. Xia, F. Chen, J. Li, N. Tao, Measurement of the quantum capacitance of graphene, Nat. Nanotechnol. 4 (2009) 505–509, https://doi.org/10.1038/nnano.2009.177.

[115] N.F. Mott, E.A. Davis, Electronic Processes in Non-crystalline Materials, Clarednon Press, Oxford. 1971, p. 591, https://doi.org/10.1016/0040-6090(72)90068-5.

[116] S. Das Sarma, S. Adam, E.H. Hwang, E. Rossi, Electronic transport in two dimensional graphene, ArXiv Prepr. ArXiv1003. 4731 (2010) 1–85, https://doi.org/10.1103/RevModPhys.83.407.

[117] R. Kumar, A. Pérez del Pino, S. Sahoo, R.K. Singh, W.K. Tan, K.K. Kar, A. Matsuda, E. Joanni, Laser processing of graphene and related materials for energy storage: state of the art and future prospects, Prog. Energy Combust. Sci. 91 (2022) 100981, https://doi.org/10.1016/j.pecs.2021.100981.

[118] P. Suvarnaphaet, S. Pechprasarn, Graphene-based materials for biosensors: a review, Sensors 17 (2017) 2161, https://doi.org/10.3390/s17102161.

[119] C. Berger, Z. Song, T. Li, X. Li, A.Y. Ogbazghi, R. Feng, Z. Dai, N. Alexei, M.E.H. Conrad, P.N. First, W.A. De Heer, Ultrathin epitaxial graphite: 2D electron gas properties and a route toward graphene-based nanoelectronics, J. Phys. Chem. B 108 (2004) 19912–19916, https://doi.org/10.1021/jp040650f.

[120] J. Tuček, P. Błoński, J. Ugolotti, A.K. Swain, T. Enoki, R. Zbořil, Emerging chemical strategies for imprinting magnetism in graphene and related 2D materials for spintronic and biomedical applications, Chem. Soc. Rev. 47 (2018) 3899–3990, https://doi.org/10.1039/C7CS00288B.

[121] R. Kumar, S. Sahoo, E. Joanni, R.K. Singh, W.K. Tan, K.K. Kar, A. Matsuda, Recent progress in the synthesis of graphene and derived materials for next generation electrodes of high performance lithium ion batteries, Prog. Energy Combust. Sci. 75 (2019) 100786, https://doi.org/10.1016/j.pecs.2019.100786.

[122] K. Jensen, K. Kim, A. Zettl, An atomic-resolution nanomechanical mass sensor, Nat. Nanotechnol. 3 (2008) 533–537, https://doi.org/10.1038/nnano.2008.200.

[123] X. Wang, X. Qi, Z. Lin, D. Battocchi, Graphene reinforced composites as protective coatings for oil and gas pipelines, Nanomaterials 8 (2018) 1005, https://doi.org/10.3390/nano8121005.

[124] X. Wang, F. Tang, X. Qi, Z. Lin, Mechanical, electrochemical, and durability behavior of graphene nanoplatelet loaded epoxy-resin composite coatings, Compos. B Eng. 176 (2019) 107103, https://doi.org/10.1016/j.compositesb.2019.107103.

[125] X. Wang, F. Tang, Q. Cao, X. Qi, M. Pearson, M. Li, H. Pan, Z. Zhang, Z. Lin, Comparative study of three carbon additives: carbon nanotubes, graphene, and fullerene-C60, for synthesizing enhanced polymer nanocomposites, Nanomaterials 10 (2020) 838, https://doi.org/10.3390/nano10050838.

[126] P. Gong, Y. Li, G. Zhang, Enhancing anti-corrosion property of novolac vinyl ester coatings on mild steel through introduction of fluoric acrylic monomer and β-Si3N4 nanoparticles, Colloids Surfaces A Physicochem. Eng. Asp. 635 (2022) 128075, https://doi.org/10.1016/j.colsurfa.2021.128075.